Appendix

Table of Contents

Appendix Figure S1. Glut1 is major glucose transporter in ECs.

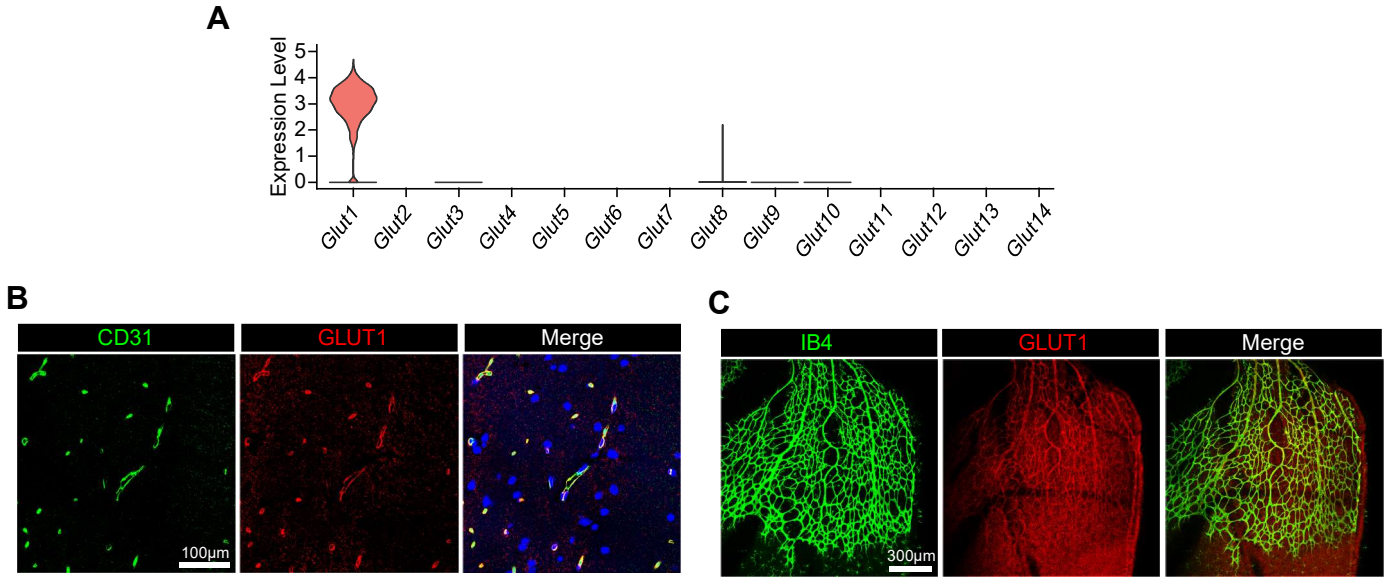

A. Violin plots showing the expression of glucose transporters in brain endothelial cells (EC atlas). Note that Glut1 shows the most abundant expression in ECs. **B.** Confocal images showing GLUT1 expression (red) together with CD31 (green) in the adult brain vasculature. **C.** Confocal images showing GLUT1 expression (red) together with Isolectin-B4 (green) in the P6 retinal vasculature.

Appendix Figure S2. Deficiency of Glut1 in EC inhibits glucose uptake and glycolysis.

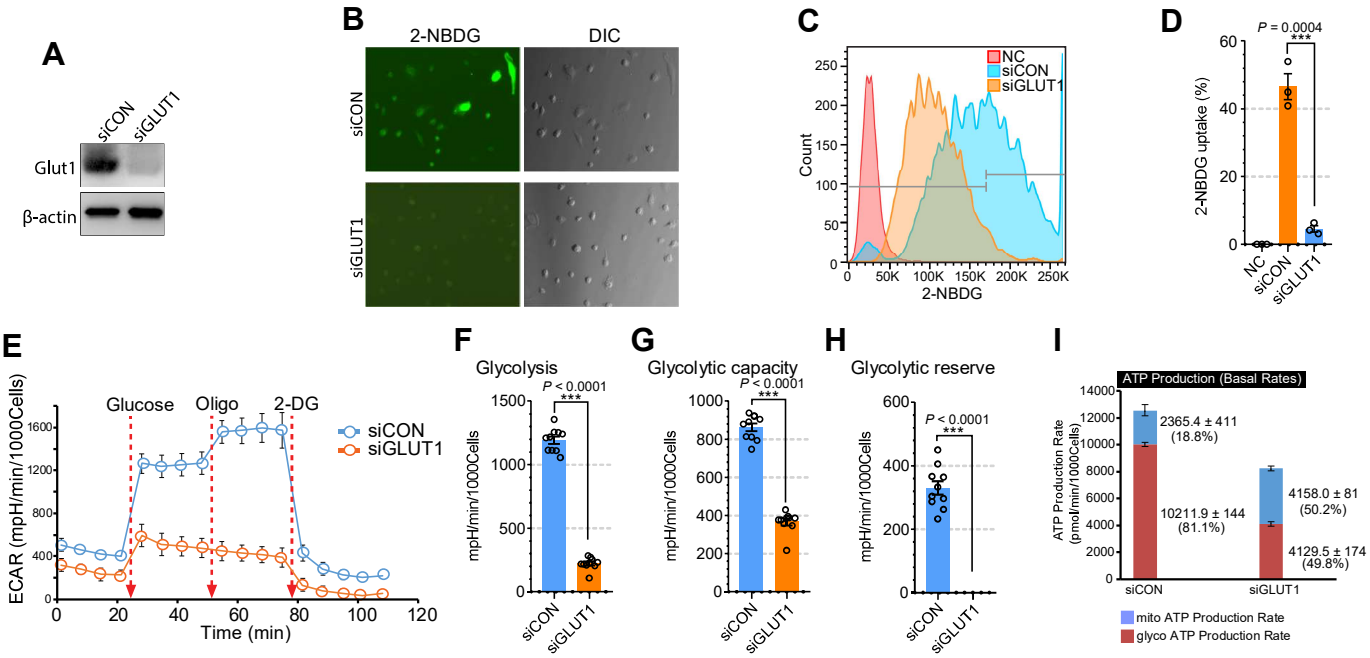

A. Western blot analysis for GLUT1 siRNA efficiency. **B.** Fluorescence assessment of 2-NBDG uptake in siRNA treated HUVECs (top : siCON, bottom : siGLUT1). **C.** Cytofluorescence assessment of 2-NBDG uptake in HUVECs (red : 2-NBDG untreated EC, blue : siCON-treated EC, orange : siGLUT1-treated EC). **D.** Quantification of 2-NBDG uptake by flow cytometry. Data are mean±SEM from 3 separate experiments. **E.** Extracellular acidification rate (ECAR) analysis in siCON and siGlut1-treated HUVECs. Before analysis, the media was replaced with glucose-free media. After 4 times of measurement, indicated nutrient/inhibitors (glucose (5mM), oligomycin (oligo; 3μM) and 2-deoxy glucose (2-DG; 100mM)) were added subsequently. (*n*=10) **F.** Quantification of glycolysis (induced) from ECAR analysis with siCON or siGLUT1-treated HUVECs. (*n*=10) **G.** Quantification of glycolytic capacity from ECAR analysis with siCON or siGLUT1-treated HUVECs. (*n*=10). **H.** Quantification of glycolytic reserve from ECAR analysis with siCON or siGLUT1-treated HUVECs. (*n*=10) **I.** ATP production rate from mitochondria (mitoATP) and glycolysis (glycoATP) in siCON or siGLUT1-treated HUVECs. Bar plots show ATP production rate from glycolysis (brown) and mitochondrial respiration (blue). Note that siGLUT1-treated HUVECs were less glycolytic than siCON-treated HUVECs. (*n*=17)

Appendix Figure S3. Glut1 is essential for endothelial proliferation and migration.

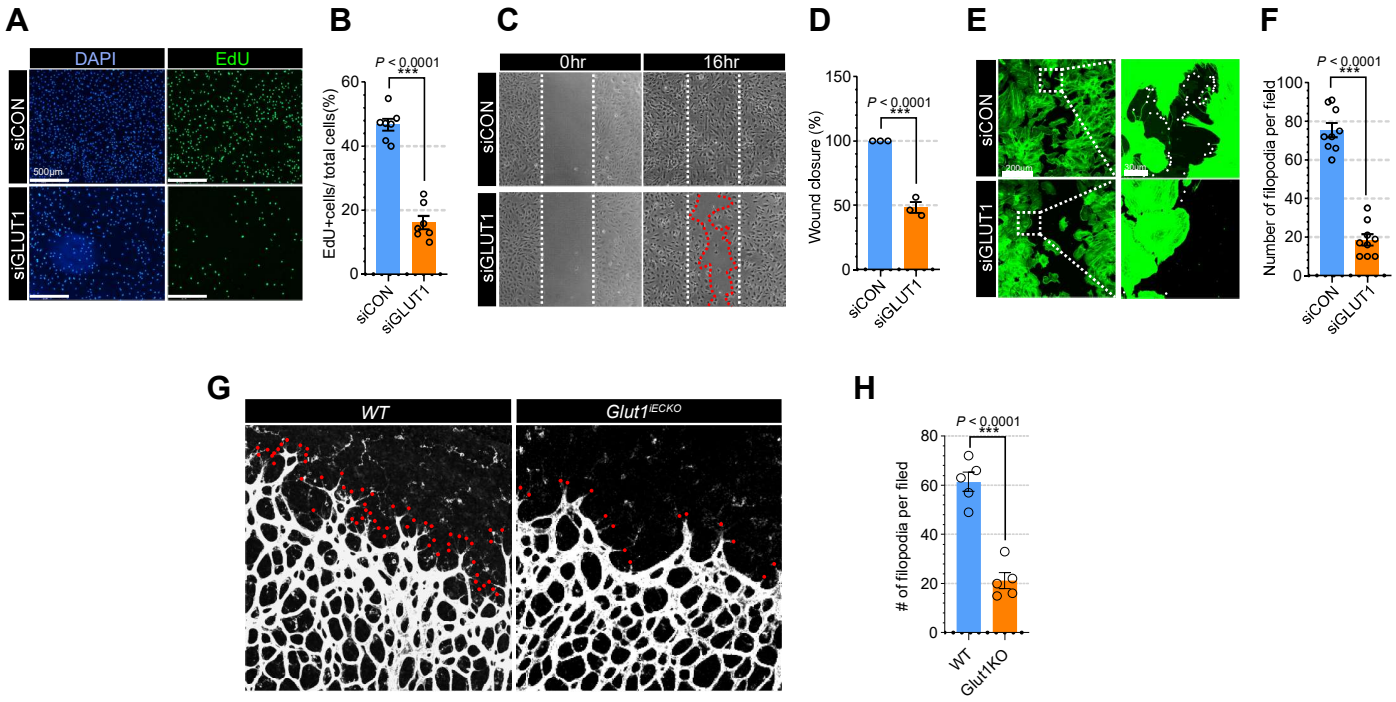

A. EdU staining showing proliferation acitivity in siCON (top) and siGLUT1 (bottom)-treated HUVECs. (EdU : green, DAPI : blue) **B.** Quantification on the number of EdU positive cells in siCON (blue) and siGLUT1 (orange)-treated HUVECs. (*n*=7) **C.** Representative images from wound healing assay using siCON (top) and siGLUT1 (bottom)-treated HUVECs. Images were taken immediately after scratching the cultures 0hr (left) and 16hr (right) later. White dotted lines indicate wounded area at 0hr and red dotted lines show uncovered area in siGLUT1-treated HUVECs at 16hr. **D.** Quantification of the wound healing assay using siCON (blue) and siGLUT1 (orange)-treated HUVECs. (*n*=3) **E.** Phalloidin staining (green) showing the number of filopodia (white dots in right panel) in siCON and siGLUT1 treated HUVECs. White dotted rectangles in the left panels were shown at higher magnification in the right panels. **F.** Quantification of the number of filopodia in siCON (blue) and siGLUT1 (orange)-treated HUVECs. (*n*=9) **G.** Representative confocal images (IB4: white) showing filopodia (red dots) in retinal vasculature from *WT* (left) and *Glut1*^{iECKO} (right) mice. **H.** Quantification of the number of filopodia in *WT* (left) and *Glut1*^{iECKO} (right) mice. (*n*=5)

Appendix Figure S4. Glut1 deletion strategy in ECs and deletion efficiency.

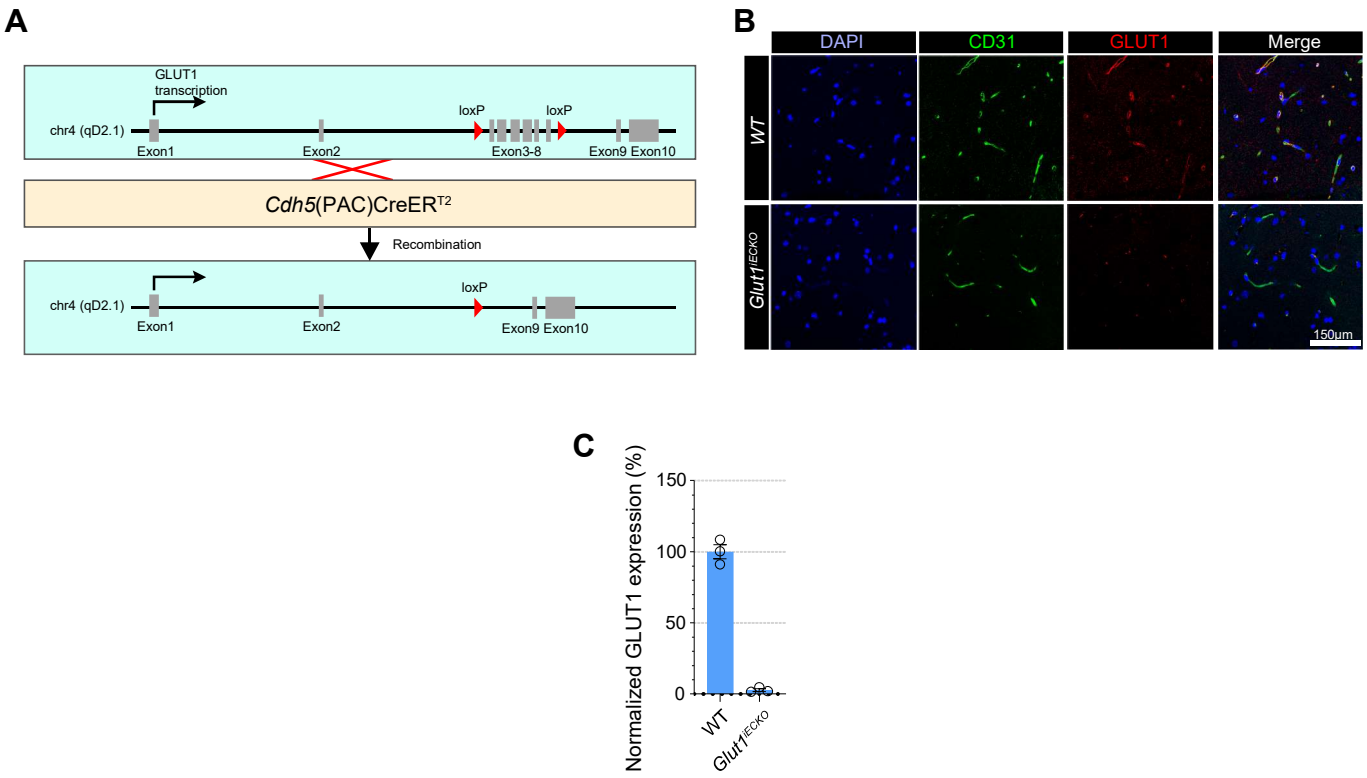

A. Schematic illustration of the strategy for endothelial specific inducible *Glut1* knockout mice. Genomic region of *Glut1* gene flanked by two loxP sites was removes by *Cdh5* promoter (endothelial specific promoter) driven Cre recombinase. **B.** Immunostaining showing GLUT1 expression in the brain vasculature of WT and *Glut1*^{iECKO} mice. (DAPI : green, CD31 : green, GLUT1 : red) **C.** Quantification of GLUT1 RNA expression level in isolated brain ECs from WT and *Glut1*^{iECKO} mice. (*n*=3)

Appendix Figure S5. Depletion of GLUT1 in EC shows delayed angiogenesis and results in lethality.

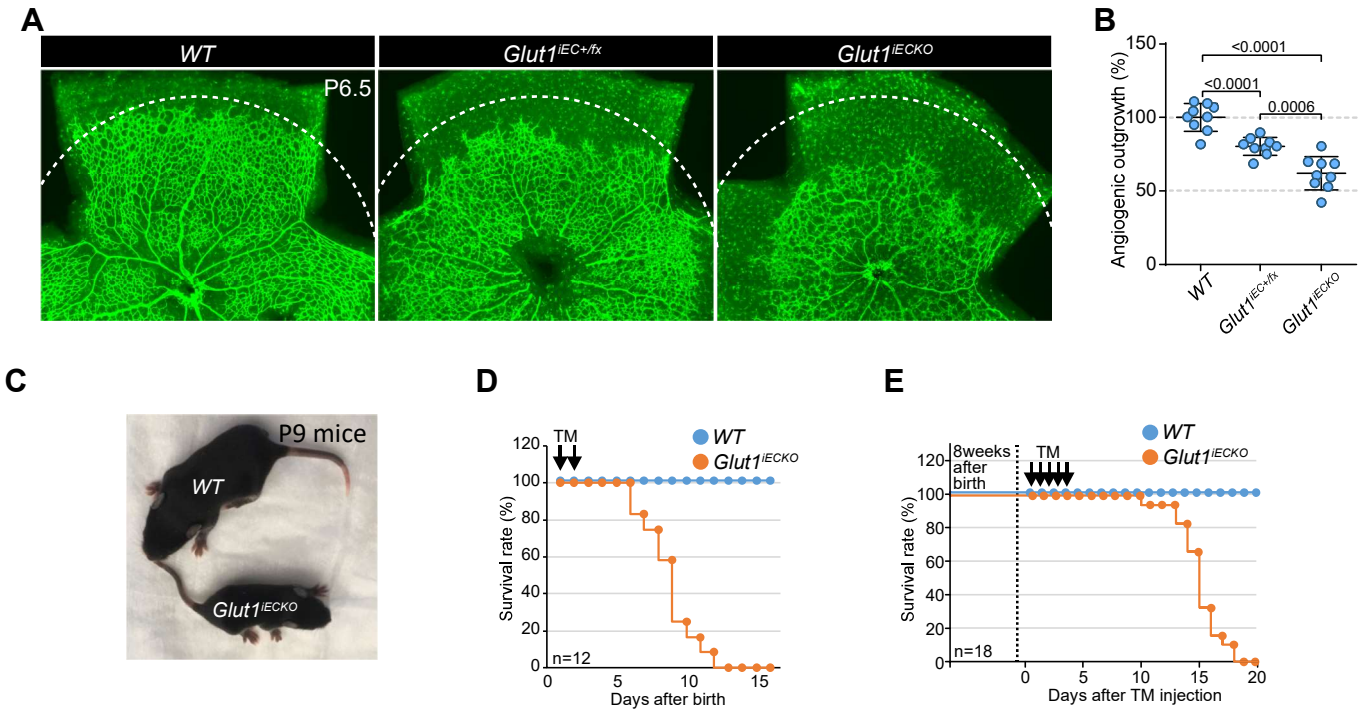

A. Isolectin B4 staining (green) showing the vascular outgrowth of P6.5 retinal vasculature of WT, *Glut1*^{iEChet} and *Glut1*^{iECKO} mice. White dotted circles indicate the size of vascular outgrowth from *WT* retina for comparison. **B.** Quantification of vascular outgrowth of retinal vasculature from WT, *Glut1*^{iEChet} and *Glut1*^{iECKO} mice. (*n*=9) **C.** Physical appearance of *Glut1*^{iECKO} and its *WT* littermate at P9 after tamoxifen injection at P1 and P2. *Glut1*^{iECKO} mice typically appear smaller in size **D.** Kaplan-Meier survival curve of *WT* (blue) and *Glut1*^{iECKO} (orange) after tamoxifen injection at P1 and P2. (*n*=12) Arrows indicate the tamoxifen injection point. **E.** Kaplan-Meier survival curve of *WT* (blue) and *Glut1*^{iECKO} (orange) after tamoxifen injection at P60. (*n*=18) Arrows indicate the tamoxifen injection point.

Appendix Figure S6. Loss of GLUT1 in EC decreases pericyte coverage in mature vasculature.

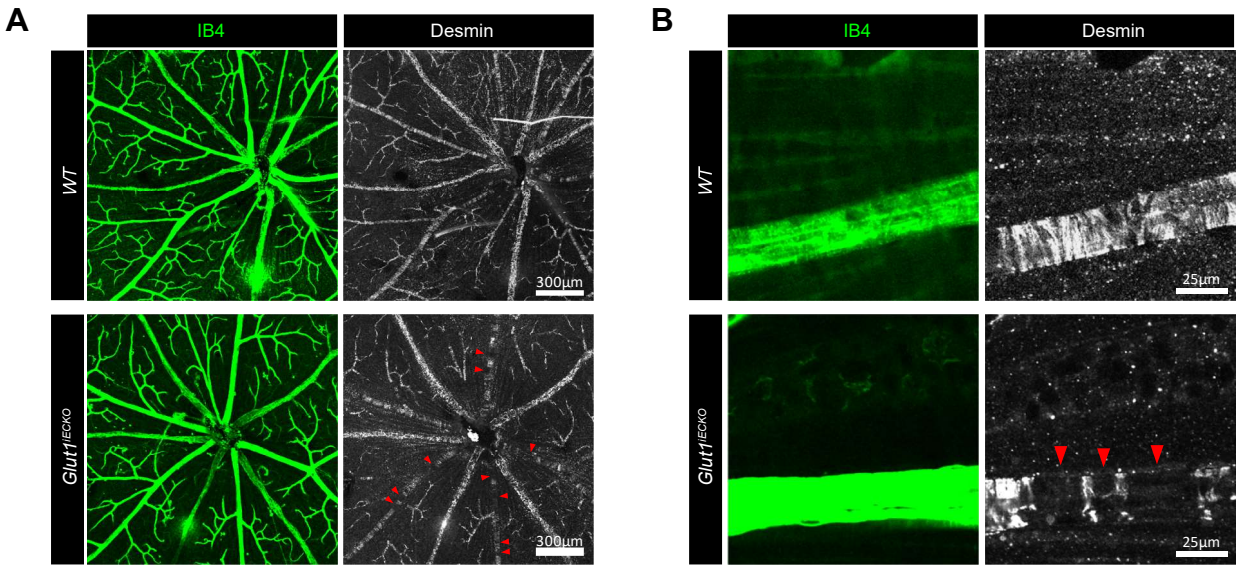

Retinal whole mount immunostaining for Isolectin-B4 (green) and Desmin (white) in adult *WT* (top panel) and *Glut1*^{iECKO} (bottom panel) mice showing pericyte coverage in the vasculature. Red arrowheads indicate the area with discontinuous pericyte coverage. Left **(A)** and right panels **(B)** show representative images with 10x or 63x magnification, respectively.

Appendix Figure S7. Loss of GLUT1 in EC does not have effect on endothelial permeability.

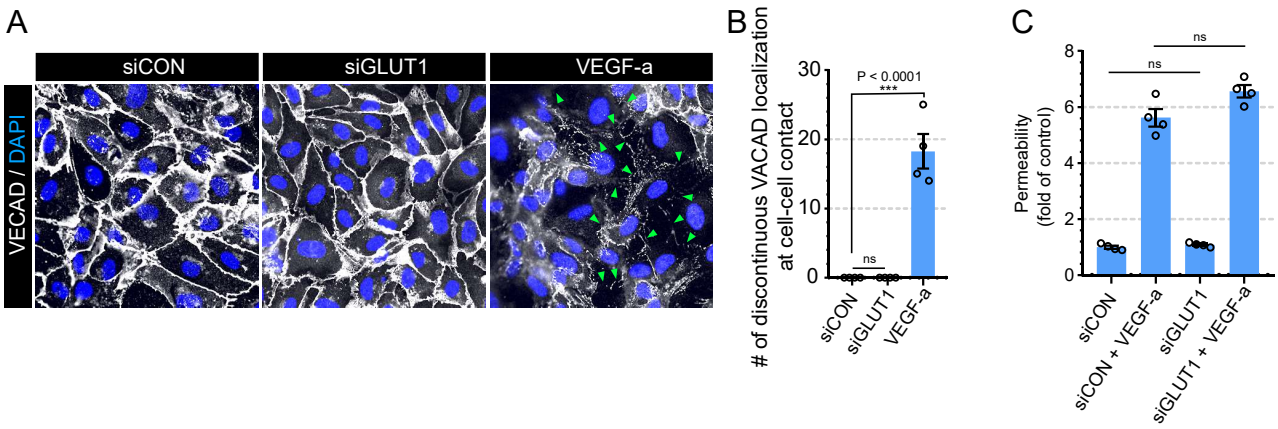

A. Representative images showing DAPI and VE-cadherin (VECAD) immunostaining in siCON, siGLUT1 or VEGF-a (50ng/mL) treated BMECs. Green arrowheads indicate discontinuous VECAD staining at cell-cell contact sites. Note that GLUT1 silencing did not show any change of VECAD localization, but VEGF-a treatment induced discontinuous VECAD localization at cell-cell contact sites. **B.** Quantification of discontinuous VECAD staining at cell-cell contact sites in siCON, siGLUT1 or VAGF-a treated BMECs. (*n*=5). **C.** Quantification of in-vitro permeability assay with siCON or siGLUT1 treated BMECs using FITC-dextran in a transwell. (*n*=4)

Appendix Figure S8. MS/MS product ion spectra of analytes.

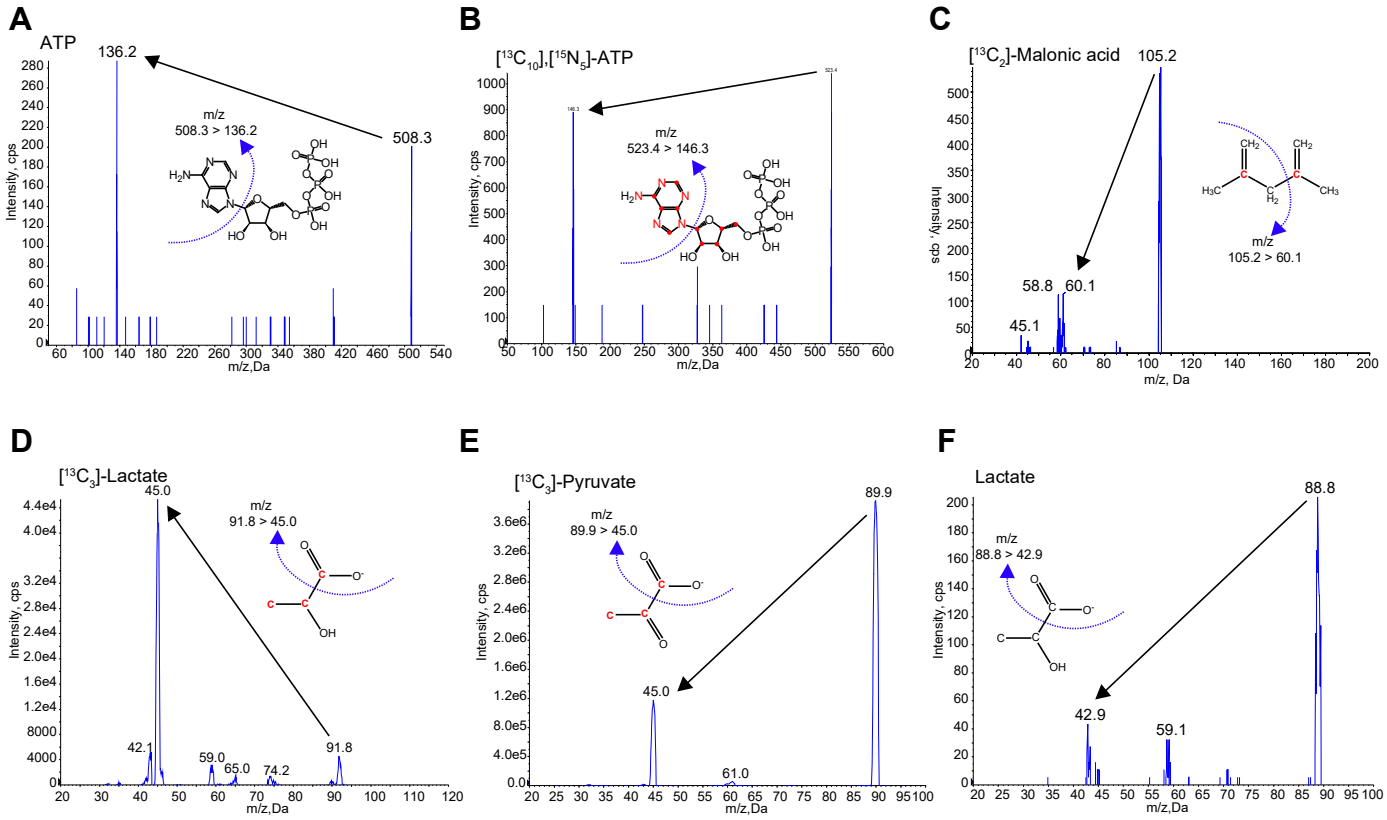

MS/MS product ion spectra showing the molecular weight of mother/daughter ions and fragmentation pattern of **A.** ATP (*m/z* : 508.3 → 136.2), **B.** [$^{13}C_{10}$],[$^{15}N_3$]-ATP (*m/z* : 523.4 → 146.3), **C.** [$^{13}C_3$]-Malonic acid (*m/z* : 104.8 → 60.1), **D.** [$^{13}C_3$]-Lactate (*m/z* : 91.8 → 45.0), **E.** [$^{13}C_3$]-pyruvate (*m/z* : 89.9 → 45.0) and **F.** Lactate (*m/z* : 88.8 → 42.9). Those molecular weight were used for the quantification of each metabolite using LC-MS/MS.

Appendix Figure S9. Administration of MCT1 inhibitor decreases lactate level in the CSF and alters BBB permeability.

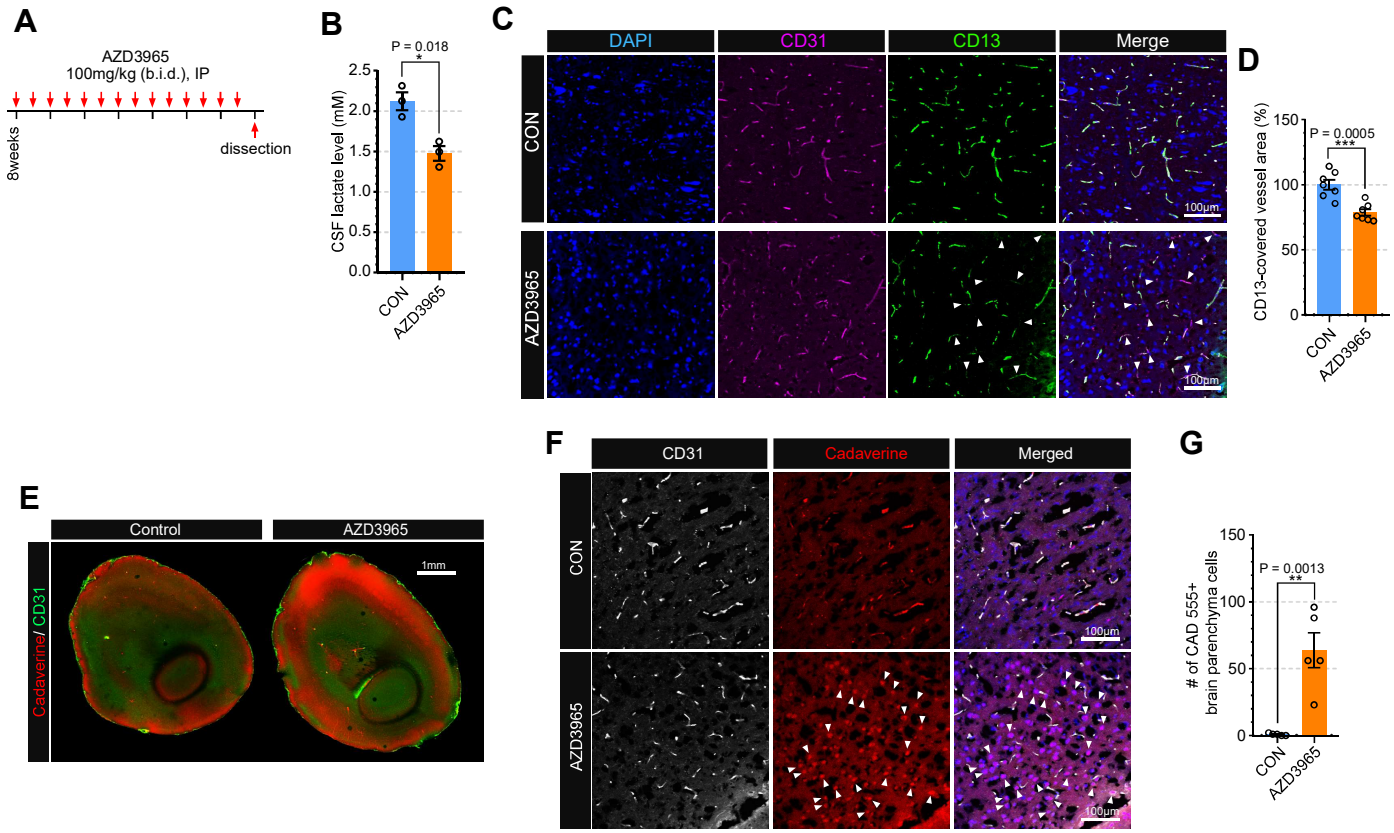

A. Schematic illustration of the strategy for MCT1 inhibitor (AZD3965) administration in adult mice (8-weeks old). Mice were treated with 100 mg/kg BID (twice a day) AZD3965 or vehicle control by intraperitoneal (IP) injection for 7 days and then sacrificed for further analysis. **B.** Quantification of lactate level in CSF of vehicle control (blue) or AZD3965 (orange)-treated mice. (*n*=3) **C.** Representative confocal images for DAPI (blue), CD31 (purple) and CD13 (green) staining with brain section (vibratome) of vehicle control (upper panel) or AZD3965 (bottom panel)-treated mice. White arrowheads indicate pericyte(CD13^{+})-deficient vessels. **D.** Quantification of CD13+ pericyte covered brain vasculature of vehicle control (blue) or AZD3965 (orange)-treated mice. (*n*=7) **E.** Permeability assay using vibratome section showing the leakage of retro-orbital injected cadaverine dye (red) and CD31 staining (green) in the brain of vehicle control (left) or AZD3965 (right)-treated mice. **F.** Representative confocal images for CD31 (white) and cadaverine (red) staining with brain section (vibratome) of vehicle control (upper panel) or AZD3965 (bottom panel)-treated mice. White arrowheads indicate cadaverine-accumulated brain parenchymal cells. **G.** Quantification of the number of cadaverine-positive brain parenchyma cells in vehicle control (blue) or AZD3965 (orange)-treated mice. (*n*=5)

Appendix Figure S10. CSF glucose level is decreased in *Glut1*^{iECKO} mice.

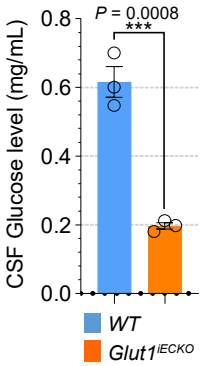

Quantification of CSF glucose level in *WT* (blue) and *Glut1*^{iECKO} (orange) mice. (*n*=3)